

Comparative study on small-scale HPs for decentral DHW preparation in multi-family buildings

William Monteleone¹, Fabian Ochs¹

¹ Unit for Energy Efficient Building, University of Innsbruck, Austria

Abstract

In renovated multi-family buildings, domestic hot water preparation is still predominantly supplied by gas-fired or electric boilers. Where centralized solutions cannot be adopted, flat-wise compact heat pump solutions can contribute substantially to the decarbonization of the building stock and reduce the invasiveness of the installation, but an experiments-based comparative study of different decentral hydronic concepts is missing in the literature. Within this work, three heat pumps based solutions for decentral domestic hot water preparation were tested and their dynamic behavior with a predefined tapping pattern was observed. The results highlighted that the use of a mantle heat exchanger in common boiler heat pumps results in longer charging intervals and increased electricity consumption. Through simulations, the monthly performance of the air-source systems was evaluated and indicated a mini-split solution as the most efficient, with a yearly performance factor of 2.5.

Keywords: Decentral DHW preparation, Compact heat pumps, serial renovation, multi-family buildings

1. Introduction

Space heating (SH) and domestic hot water (DHW) preparation in multi-family buildings (MFBs) are still heavily based on fossil fuels or inefficient technologies (IEA, 2022). To achieve the climate-neutrality targets of the European Union (EU) concerning the building stock by 2050 (European Commission, 2021), an increase in the renovation rate is required as well as a swift transition to efficient and sustainable heating systems. Heat Pumps (HPs) will play a decisive role in the decarbonization of the building sector (IEA, 2022) but their implementation in MFBs often faces technical and non-technical challenges, among them source-accessibility, installation space requirements, noise as well as invasiveness (Cozza et al., 2022). Where centralized HPs cannot be adopted, flat-wise HP solutions for DHW preparation are promising candidates to replace gas-fired boilers or E-boilers but their investment costs are usually higher than traditional technologies (Gustafsson et al., 2017). Within this work, three HP-based solutions for decentral DHW preparation will be evaluated, consisting of a façade-integrated mini-split air-to-water HP (Monteleone et al., 2024), a air-source boiler HP and a return flow water-to-water HP. The first solution was investigated within the research projects “FitNeS” (FFG (Austrian Research Promotion Agency), 2023) and “PhaseOut” (FFG (Austrian Research Promotion Agency), 2024), while the others are commercial solutions already available on the market. Prefabricated façade elements allow on one hand the improvement of the building envelope and on the other hand a fast, cost-effective replacement of fossil-based technologies. First, the three solutions are tested in the laboratory over a cycle of 24 hours and variable heat source temperature to assess their dynamic performance. Based on the measurements, performance maps depending on source and sink temperature were obtained for the air-source HPs and a yearly simulation was performed for the climate of Innsbruck in the Simulink environment with the use of the Carnot Toolbox (Solar-Institut Juelich FH Aachen, 2018). Out of the simulations, a yearly system performance factor was calculated for the two air-based solutions, as well as the peak photovoltaic (PV) power necessary to cover 50% of the yearly HP electric consumption.

2. Methodology

The hydronic systems which will be analyzed within this work are depicted schematically in Figure 1 to Figure 3. Figure 1 shows a semi-central system with a central HP supplying the SH demand of the building and a decentral air-source boiler HP for DHW preparation. The heat source (air) can be either room air or outside air

by means of a duct. In Figure 2 a system with a central HP for SH and a decentral return flow HP for DHW is shown. The return flow HP uses the return of the SH as a heat source to heat up a storage tank (integrated within the HP casing). Then, in Figure 3, the decentral DHW preparation is provided by means of a 1.5 kW façade-integrated split air-to-water HP, as the one described in (Monteleone et al., 2024; Ochs et al., 2022). With focus only on DHW preparation, all three systems have been replicated and tested in the hydraulics laboratory of the University of Innsbruck and their dynamic behavior has been observed.

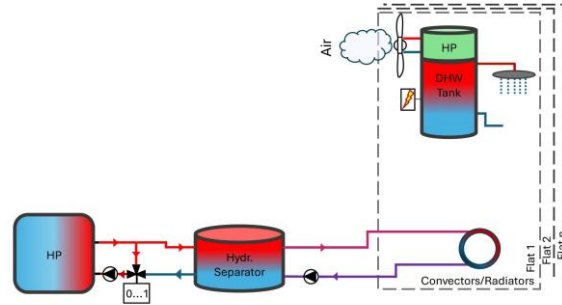


Figure 1: Conceptual scheme of a hydronic system with central HP for SH and decentral ambient air HP for DHW preparation.

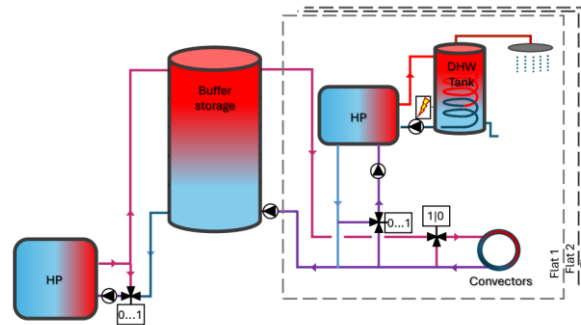


Figure 2: Conceptual scheme of a hydronic system with central HP for SH and decentral return flow HP for DHW preparation (and optionally for cooling).

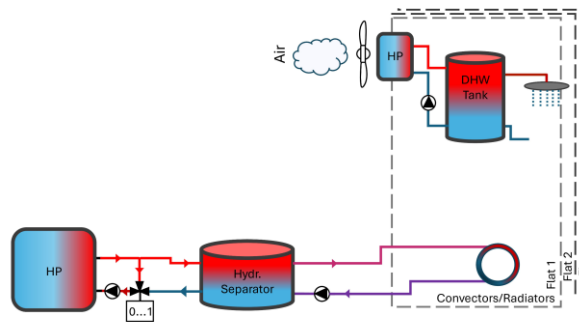


Figure 3: Conceptual scheme of a hydronic system with central HP for SH and decentral façade-integrated split air-to-water HP for DHW preparation.

2.1. Experiments

The HP-based solutions mentioned in the previous sections were tested in a double-room climate chamber. Each test room is 200 cm x 250 cm x 280 cm and is insulated with 8 cm polyurethane. Heating and cooling in each room are provided by means of water-based fan coils. The test duration is 15 hours, during which the tapping profile “M” is applied to replicate the hot water consumption of a medium-small flat (CEN/TC 113, 2017). Table 1 gives an overview of the boundary conditions applied during the measurements to each decentral HP concept for DHW preparation. The required source temperature for all air-source HP concepts is guaranteed by means of the fan coils installed in the test rooms, while a 5000 Liters water storage tank is used

as heat source for the return flow HP. The water is delivered from the heat source (i.e. 5000 Liters hot water storage tank) to the test specimen by means of an unpressurised manifold, with the possibility to control the flow rate and supply temperature by means of a mixing valve and a variable speed pump, as shown in Figure 4(a). For the ambient air-to-water boiler HP concept, the unit is installed in a room where the indoor air temperature corresponds to the requested source temperature. The tested ambient air and return flow HP are commercial units available on the market and share the same HP layout. For their test procedures, the setup depicted in Figure 4(b) was adopted.

Table 1: Boundary conditions applied during the measurements for each decentral HP concept.

Ambient air-to-water HP	
Source temperature (Room air) / [°C]	10....15....20
Source (air) volume flow / [m ³ /h]	160
Storage tank size / [Liters]	150
Return flow HP	
Source temperature (SH return) / [°C]	25....30....35 (Manufacturer's limitations)
Source (water) volume flow / [l/min]	5
Storage tank size / [Liters]	150
Façade-integrated split air-to-water HP	
Source temperature (Outdoor air) / [°C]	10....15....20
Source (air) volume flow / [m ³ /h]	350
Storage tank size / [Liters]	120

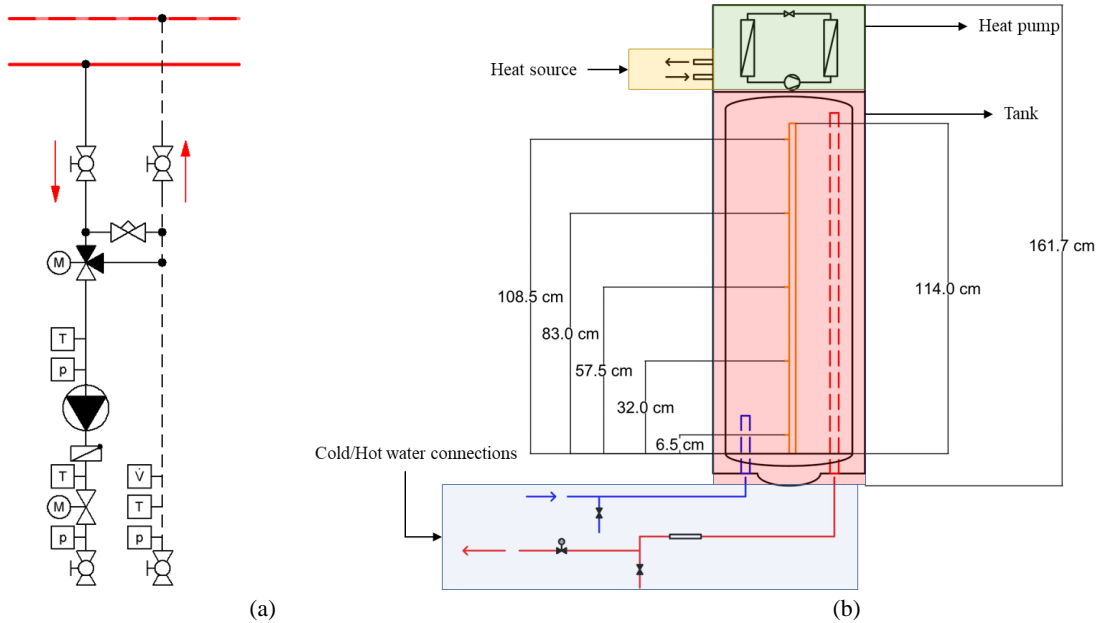


Figure 4: (a) Test infrastructure for the control of source temperature level and flow rate in the measurement of the return flow HP and (b) Test layout for the measurement of ducted air-source HP and return flow HP. The probe with 5 Pt100 sensors inside the storage tank is also shown.

Water is heated up by means of a mantle heat exchanger installed between the tank lining and the insulation layer. Inside the water tank, a rod carrying 5 Pt100 temperature sensors is installed in order to monitor the thermal stratification. Both HP models are provided with an electric back-up heater, which however is disconnected during the measurements. To apply the tapping profile, a magnetic 2-way valve is used. The (tapped) water volume flow is detected by means of a magnetic flow meter (MFM). The measurement starts with a fully charged storage with a setpoint temperature of 55 °C and the tapping cycle is initiated 30 seconds afterwards. After the completion of the full tapping cycle, the measurement is stopped. In the case of the mini-split air-to-water HP, the outdoor unit is placed in the room replicating the outdoor air conditions, while the remaining infrastructure is placed in the ambient room at a temperature of 20 °C. The test layout highlighted in Figure 5 is adopted, similar to the one used for the previous HP concepts. Three temperature sensors are installed within the DHW storage, 5 cm, 36 cm and 64 cm from the top edge of the tank respectively. The flush valve on the cold water side is kept open for the whole duration of the test to guarantee a possibly constant

freshwater temperature. Figure 6(a), (b) and (c) depict the double room climate chamber used for the measurements, the outdoor unit of the tested mini-split air-to-water HP and its layout when integrated in a test façade.

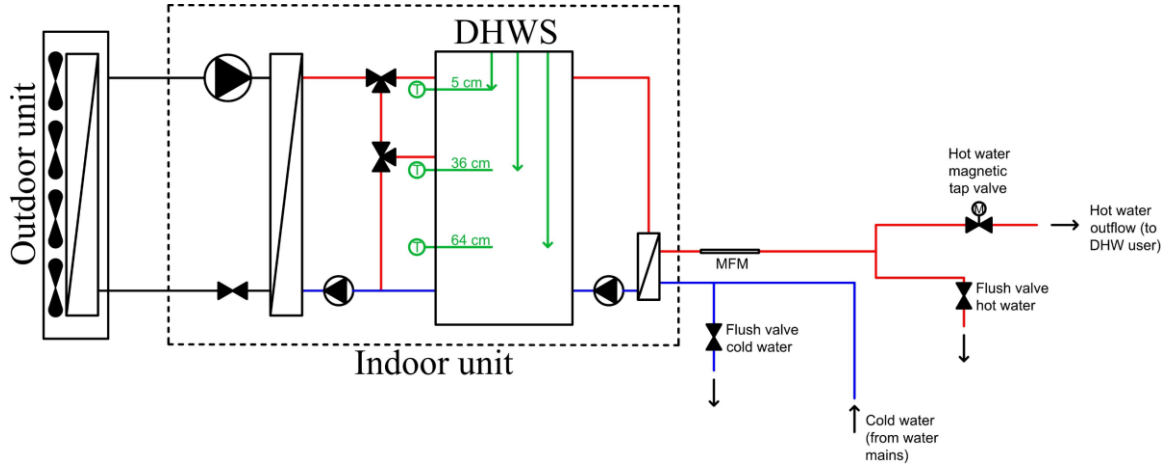


Figure 5: Test setup for a mini-split air-to-water HP with integrated DHW storage.

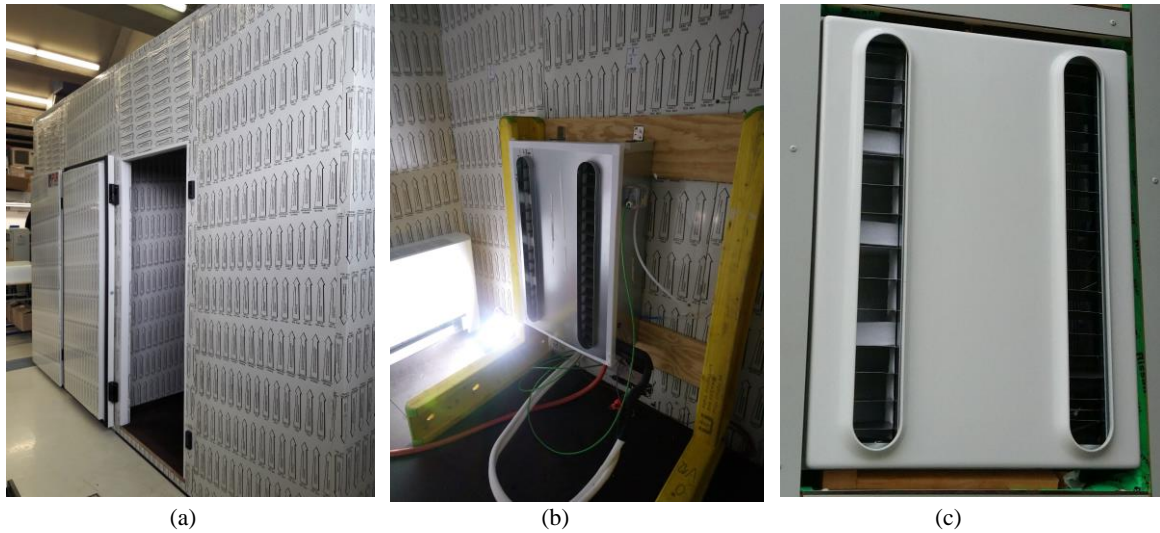


Figure 6: (a) Double-room insulated climate chamber used for the testing of air-to-water and water-to-water HPs, (b) Outdoor unit of the tested (façade-integrated) mini split air-to-water HP in the chamber and (c) outdoor unit of the mini split HP integrated in a test façade.

The performance of each HP concept is evaluated by means of the following definition of COP:

$$COP_{DHW} = \frac{Q_{DHW}}{Q_{el,HP}} \quad (\text{eq. 1})$$

Where Q_{DHW} is the energy delivered to the DHW user in [kWh_{th}] and $Q_{el,HP}$ the electricity supplied to the HP during the whole measurement cycle in [kWh_{el}].

To produce the performance maps for each HP, first the measurement data from the HP refrigerant cycle are retrieved. For ambient air and for the return flow HPs, the measurement setup represented in Figure 7(a) was available, with four temperature sensors installed within the refrigerant cycle, at the entrance and at the exit of condenser and evaporator respectively. Additionally, the electric power consumption of the compressor is measured, as well as the source and sink temperatures. For the mini-split HP, a more detailed setup (see Figure 7(b)) was used.

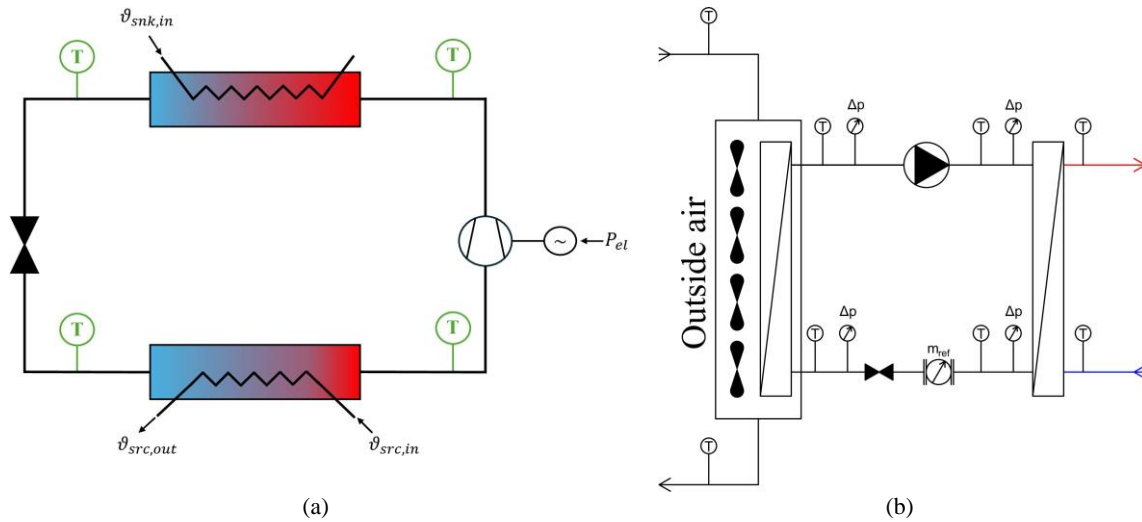


Figure 7: Schematic representation of the refrigerant cycle of a generic HP with the position of the temperature sensors.

For the tests involving the façade-integrated split HP, the pressure levels and the refrigerant mass flow are also available. The measured data are then fed to the refrigerant cycle model described in (Monteleone et al., 2024) to complete the missing information and generate the performance maps for each HP concept. The ambient air HP, as well as the return flow HP, feature the same vertical rotary-type single-speed compressor with a displacement volume of 5.6 cm^3 . On the other hand, the mini-split HP uses a horizontal rotary-type single-speed compressor but with a displacement volume of 12.7 cm^3 .

2.2. Simulations

For the DHW preparation in minimal invasive renovations, the HP concepts of Figure 1 and Figure 3 were further investigated in a dynamic simulation study within the simulation environment of MATLAB+Simulink (Mathworks, 2022) with the use of the CARNOT toolbox (Solar-Institut Juelich FH Aachen, 2018). The aim of the simulation study is to evaluate the annual performance of the investigated systems for a single flat in the climate of Innsbruck, Austria. However, instead of considering ambient air as heat source for the system in Figure 1, a ducted variant (with outdoor air as heat source) was selected for the simulation study. This was done in order to guarantee the same ambient boundary conditions to both simulated systems and focus more on the dynamic performance of the presented HP concepts. A daily “M” tapping profile was assumed for all the simulation studies, with a storage temperature setpoint of $55 \text{ }^\circ\text{C}$ and freshwater temperature equal to $13 \text{ }^\circ\text{C}$. The same tank sizes presented in Table 1 were adopted for the simulation study. The heat transfer coefficient of the storage envelope was chosen to obtain a tank with energy efficiency class ErP “B” (The European Parliament and the Council of the European Union, 2009). In the modelled system shown in Figure 8(a) (ducted air-source DHW HP), one temperature sensor is used to turn on and off the HP, positioned at 70% of the storage height. The HP is turned on when the temperature measured by the sensor is 8 K lower than the setpoint and turns off when the sensor temperature is 2 K above the setpoint. In Figure 8(b) the system with a façade-integrated mini-split air-to-water HP is illustrated. The system features a façade-integrated outdoor unit housing the evaporator and four parallel axial fans, while the indoor unit includes the compressor, the condenser, the expansion valve and a 120 litres DHW storage. An 8-kW electric post-heater is considered and the delivery of the DHW demand takes place through a freshwater station. During the startup phase of the HP, the temperature of the water supplied to the storage would be lower than the temperature in the tank. For this reason, the top mixing valve in Figure 8(b) is closed entirely and water is recirculated in a loop until the temperature sensor T0 detects a water temperature higher than $52 \text{ }^\circ\text{C}$. Once the water supply temperature has reached the setpoint, the HP begins to charge the top part of the storage to guarantee comfort in case of short-term taps. Once the reserve volume of the storage is charged, the tank is heated up via the intermediate charging point. Similarly to the system presented in Figure 8(a), the HP in Figure 8(b) is controlled by means of a hysteresis controller based on the temperature sensors T1 and T2. The HP is thus turned on when the sensor T1 detects a temperature 5 K lower than the setpoint and turns off when the sensor T2 measures a temperature equal to the setpoint plus 1 K. The temperature sensors T1 and T2 are placed at 32% and 84% of the storage height respectively. On the secondary side the speed-controlled pump is modulated by means of a PID

controller to reach a comfort temperature for the DHW user of 45 °C (temperature sensor T3). For both air-source HPs, minimum and maximum operational time intervals are assigned. If the air temperature is higher than 7 °C, the HP is assigned a minimum run time of 3 minutes while there is no maximum run time. If the air temperature falls below 7 °C, a maximum run time of 80 minutes is considered, after which the HP is stopped for 10 minutes to allow for the defrosting. The degradation of the performance of the heat exchanger due to ice formation, as well as the additional electricity consumption for defrosting, are not considered within this model.

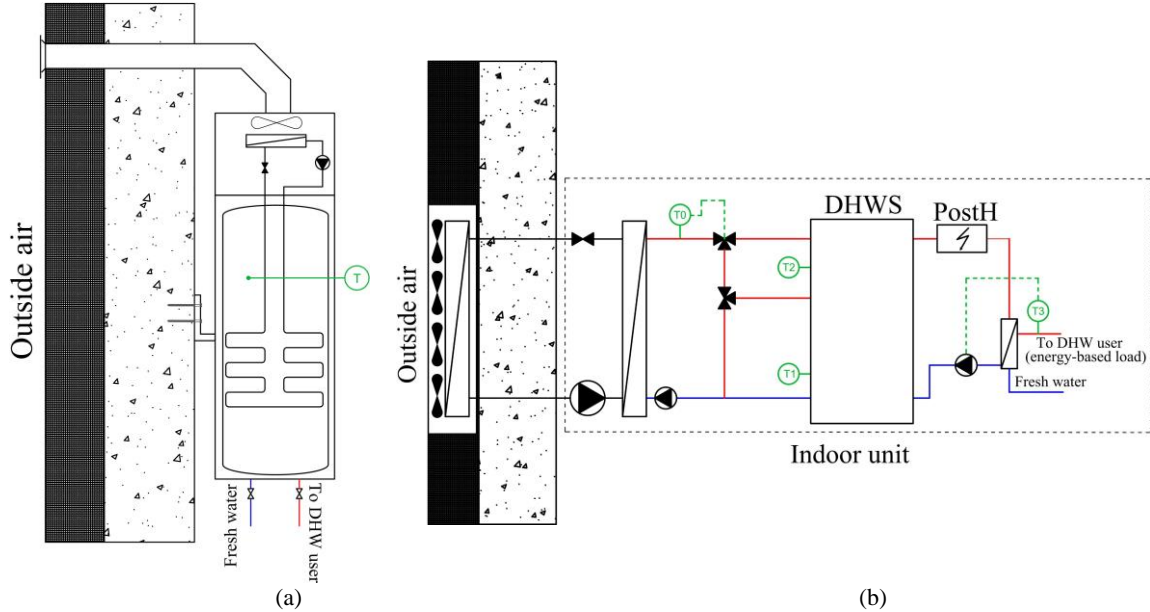


Figure 8: Modelled (a) ducted air-source DHW HP with integrated 150 litres tank and (b) façade-integrated mini-split HP with 120 litres tank, 8 kW post-heater and freshwater station.

For the evaluation of the electricity consumption covered by PV, a reference building, subjected to renovation, is considered. The reference building consists of a ground floor and four upper floors, with two-room apartments with an area of 44.0 m² and one-room apartments with an area of 37.3 m², for a total of ten flats (with reference floor plane shown in Figure 9). It is assumed that hot water consumption for each flat is the same and corresponds to the “M” profile according to the norm. While the instantaneous hot water consumption varies considerably during the day for each flat in the building, it is assumed that the monthly hot water consumption for the entire building is simply the single flat consumption in a month multiplied with the number of flats. For all simulated variants, the properties of the PV system are indicated in Table 2. The electricity consumption of the appliances as well as for circulation pumps is discarded for this study and for the evaluation of the PV coverage.



Figure 9: Floor plane of one of the one-room apartments subjected to renovation, with a floor area of 37.3 m².

Table 2: Assumptions used for the modelling of the PV system in the simulations.

Installed PV [kW _{peak}]	5 kW
Location	Roof

Slope of PV modules [°]	30 °
Azimuth [°]	0 ° (South)
Inverter efficiency [%]	96 %
Inverter standby power [W]	2 W
Maximum AC power for PV [kW]	3.8 kW

The performance of the HP concept has been evaluated for each month of the year by means of a performance factor (PF) defined as:

$$PF_{HP} = \frac{Q_{th,HP}}{Q_{el,HP} + Q_{el,PostH}} \quad (\text{eq. 2})$$

Where $Q_{th,HP}$ represents the heat delivered from the HP to the DHW storage in [kWh_{th}], $Q_{el,HP}$ the electricity consumed by the compressor and by the HP control in [kWh_{el}] and $Q_{el,PostH}$ the electricity consumption of the electric post-heater (if available) in [kWh_{el}].

The PV coverage is defined in turn as:

$$f_{PV,cover} = \frac{Q_{el,PV,AC}}{n_{flats} (Q_{el,HP} + Q_{el,PostH})} \quad (\text{eq. 3})$$

Where $Q_{el,PV,AC}$ represents the AC PV yield in [kWh_{el}] and n_{flats} the number of flats in the building.

3. Results and discussion

3.1. Experiments

In Figure 10 the measurement results for the ambient air HP at source temperature of 10 °C are shown. The top diagram depicts the profile of the temperatures detected by the 5 Pt100 sensors inserted in the probe. θ_5 represents the top sensor, θ_1 the lowest one. Then the middle diagram shows the measured HP electric power consumption, while the bottom diagram shows the tapping profile with the respective measured water volume flows.

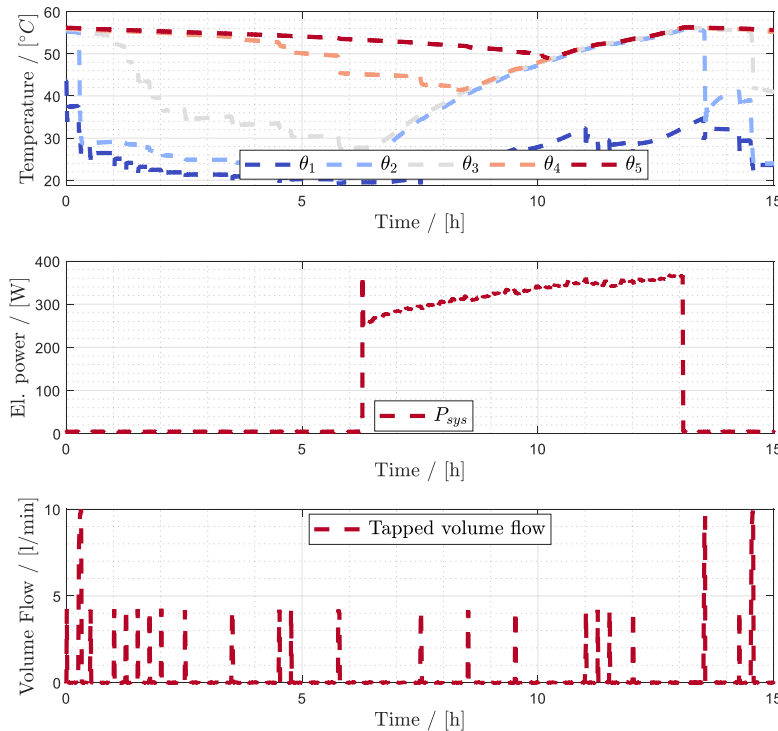


Figure 10: Dynamic test results for the ambient air HP with 10 °C ambient temperature and “M” tapping profile.

During the 15 hours of the measurement, only one charging cycle is performed by the HP which lasts for about 7 hours with an average electric power consumption of 320 W. When the charging starts, the storage is

homogeneously heated from the bottom to the top due to the presence of the mantle heat exchanger, which results in longer charging intervals and increased electricity consumption. This leads to a COP_{DHW} of 1.28, as also illustrated in Table 3. At an air temperature of 15 °C, the COP_{DHW} reaches 1.53 while it jumps to 2.85 at an air temperature of 20 °C. This behaviour was expected, since the thermal losses attributed to the storage tank are much lower at 20 °C than at 15 or 10 °C. As a consequence, the charging intervals are shorter and the electricity consumption drops from 4.03 kWh_{el} to 2.17 kWh_{el} for the whole tapping cycle.

Table 3: Summary of measurement results for the ambient air HP for DHW preparation. The cold water temperature equals 13 °C.

$\vartheta_{source} / [^{\circ}C]$	10	15	20
$Q_{DHW} / [kWh_{th}]$	6.15	6.15	6.18
$Q_{el,HP} / [kWh_{el}]$	4.83	4.03	2.17
$COP_{DHW} / [-]$	1.28	1.53	2.85

Figure 11 illustrates the measurements of the return flow HP at a source temperature of 25 °C. For this type of HP concept, the charging cycles are much shorter than in an ambient-air HP. In fact, in the diagrams presented in Figure 11, the charging interval lasts for less than 3 hours. Therefore, the resulting electricity consumption equals 1.09 kWh_{el} , as shown in Table 4. The resulting COP_{DHW} at 25 °C corresponds to 5.61, while it equals 5.84 and 6.24 at source temperatures of 30 °C and 35 °C respectively.

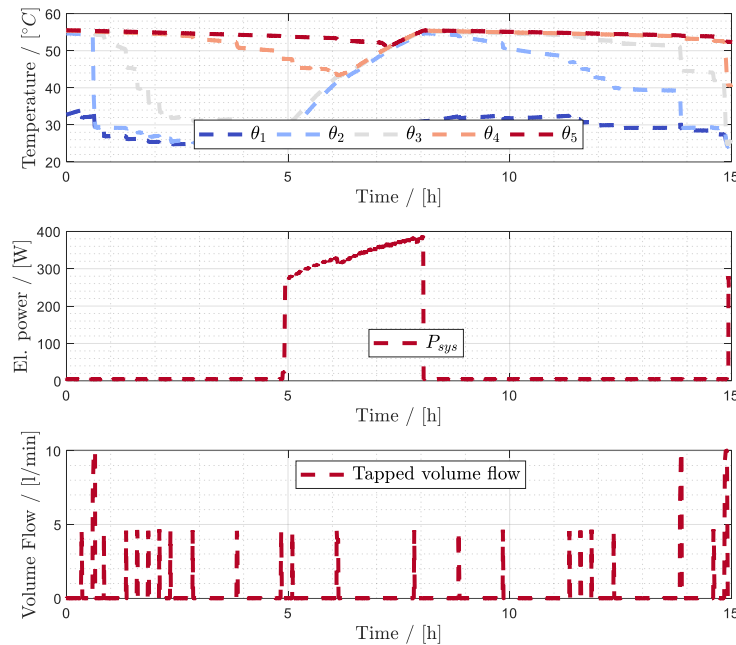


Figure 11: Dynamic test results for the return flow HP with 25 °C source temperature and “M” tapping profile.

Table 4: Summary of measurement results for the return flow HP for DHW preparation. The cold water temperature equals 13 °C.

$\vartheta_{source} / [^{\circ}C]$	25	30	35
$Q_{DHW} / [kWh_{th}]$	6.11	6.11	6.11
$Q_{el,HP} / [kWh_{el}]$	1.09	1.05	0.98
$COP_{DHW} / [-]$	5.61	5.84	6.24

Figure 12 shows then the measurement results at 10 °C air temperature for the developed mini-split air-to-water HP. During the measurement cycle, three charging cycles were observed, with a duration of about 1.5 hours each and average electric power consumption of 630 W. Since the water heated up in the condenser is directly supplied to the DHW storage (i.e. without the use of internal heat exchangers, see also Figure 5), the charging phase is also characterized by increased mixing, which causes a perturbation in the temperature of upper and medium layers. The smaller hysteresis selected for the HP control (i.e. 5 K) leads to more frequent charging cycles. Nevertheless, the electricity consumption at 10 °C air temperature corresponds to 2.12 kWh_{el} , resulting in a COP_{DHW} of 2.82 (see also Table 5). At 15 °C an electricity consumption of 1.99 kWh_{el} is detected

while at 20 °C it slightly decreases to 1.96. The resulting COP_{DHW} are therefore 3.06 and 3.11, at 15 and 20 °C respectively.

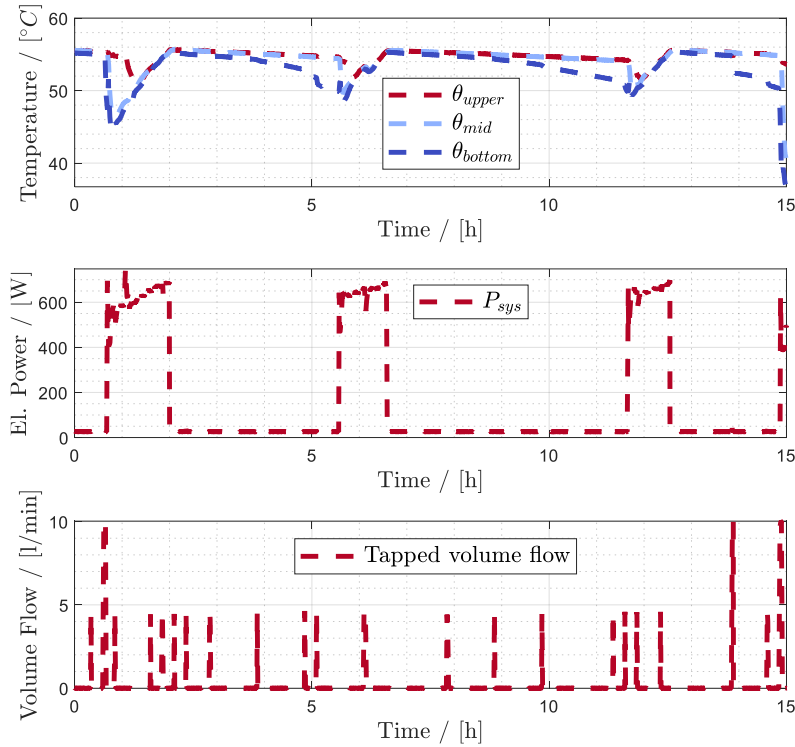


Figure 12: Dynamic test results for the mini-split HP with 10°C source temperature and “M” tapping profile.

Table 5: Summary of measurement results for the mini-split air-to-water HP for DHW preparation. The cold water temperature equals 13 °C.

$\vartheta_{source} / [^{\circ}C]$	10	15	20
$Q_{DHW} / [kWh_{th}]$	5.98	6.10	6.10
$Q_{el,HP} / [kWh_{el}]$	2.12	1.99	1.96
$COP_{DHW} / [-]$	2.82	3.06	3.11

Based on the measurements and through the use of the refrigerant cycle model presented in (Monteleone et al., 2024), the performance maps presented in Figure 13 to Figure 15 were generated. In Figure 13 it is possible to remark that the heating capacity of the ambient air HP is lowest among the analysed HP concepts, with about 900 W being delivered at A20W55. The best performance is obtained, as expected, for the return flow HP, with HP COPs well above 2.5 for source temperatures between 25 and 35 °C (see Figure 14(b)). The heating capacity however is lower than the one shown in Figure 15(a) for the mini-split HP, which in turn exhibits lower electric power consumption for the compressor and therefore lower COPs.

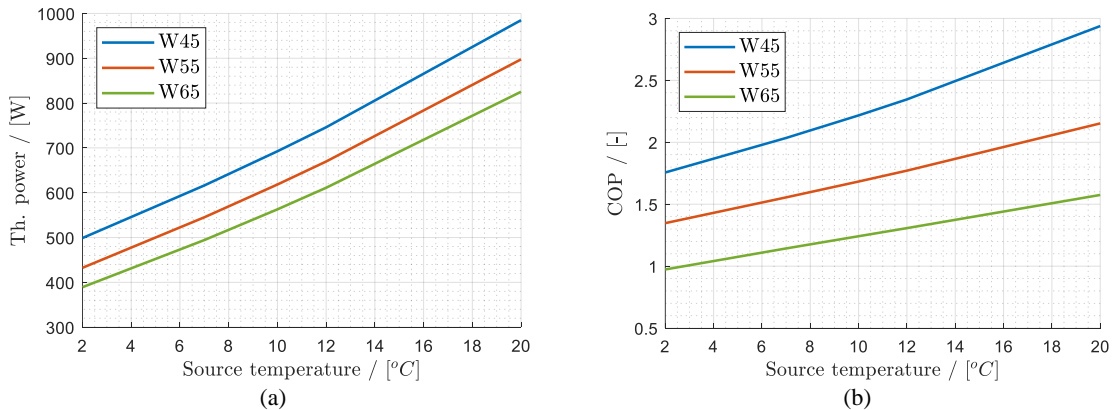


Figure 13: Performance maps of (a) condenser power and (b) COP based on measurements and refrigerant cycle model (based on (Monteleone et al., 2024)) for the ambient-air HP.

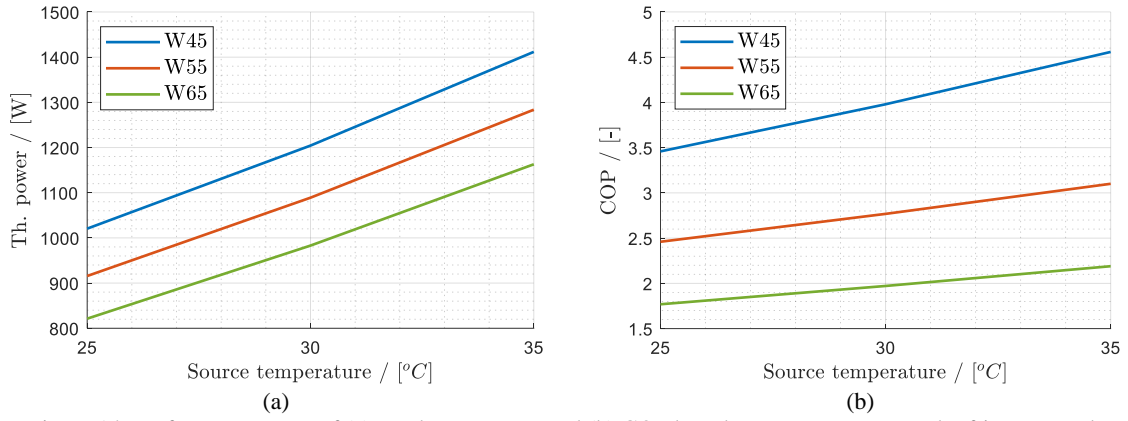


Figure 14: Performance maps of (a) condenser power and (b) COP based on measurements and refrigerant cycle model (based on (Monteleone et al., 2024)) for the return-flow HP.

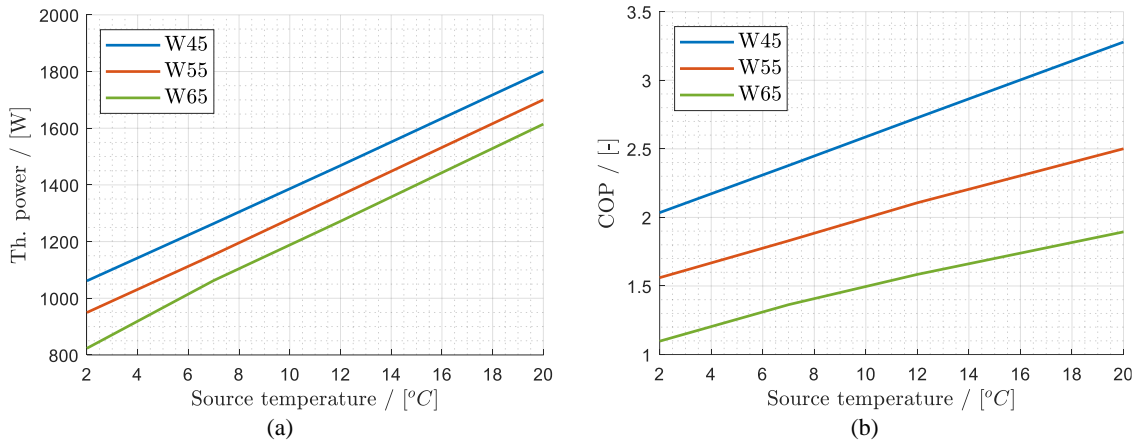


Figure 15: Performance maps of (a) condenser power and (b) COP based on measurements and refrigerant cycle model (based on (Monteleone et al., 2024)) for the mini-split air-to-water HP.

3.2. Simulations

Figure 16 shows the monthly variation of the simulated PF for DHW preparation (defined according to eq. (2)) for a system with a mini-split façade-integrated air-to-water HP (FIHP) and for a system with a ducted air-source HP (AAHP). As highlighted also in the previous section, the low capacity of air-source boiler HPs results in longer charging intervals and therefore increased electricity consumption and worse yearly performance compared to the mini-split HP. The yearly PF for a mini-split HP reaches a value of 2.50, with a maximum of 2.84 in July and a minimum of 2.11 in January. During the whole year, no post-heater operation was detected. On the other hand, for the ducted air-source HP a yearly PF of 1.99 was obtained, with a maximum of 2.49 in July and a minimum of 1.47 in January.

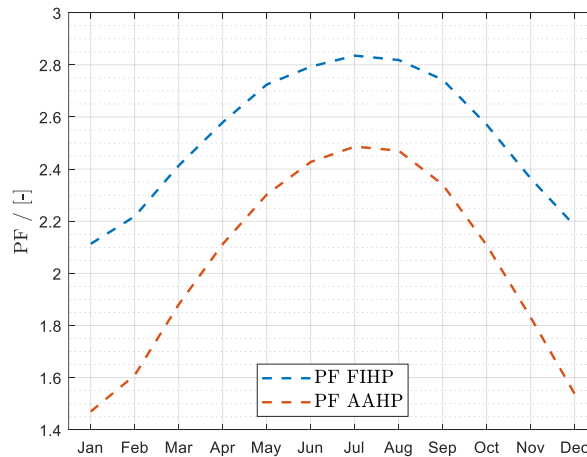


Figure 16: Simulated monthly performance factor for DHW preparation for a mini-split façade-integrated HP and for a ducted air-source HP.

The evaluation of the monthly PV yield with respect to the monthly HP electricity consumption for the reference building (see also section 2.2) yielded the results illustrated in Figure 17(a) and (b), for the mini-split HP and for the ducted air-source HP respectively. During the warmer months, the 5 kW PV supplies up to 68% of the HP electricity demand for the mini-split HP and up to 57% for the ducted boiler HP. However, a yearly coverage factor $f_{PV,cover}$ of 46% is obtained for the first, while a value of 37% is obtained for the second. Therefore, with a slightly larger PV size (if the location and the angle of each panel remain unaltered) the goal of 50% coverage can be easily reached for the mini-split HP but not for the ducted air-source HP.

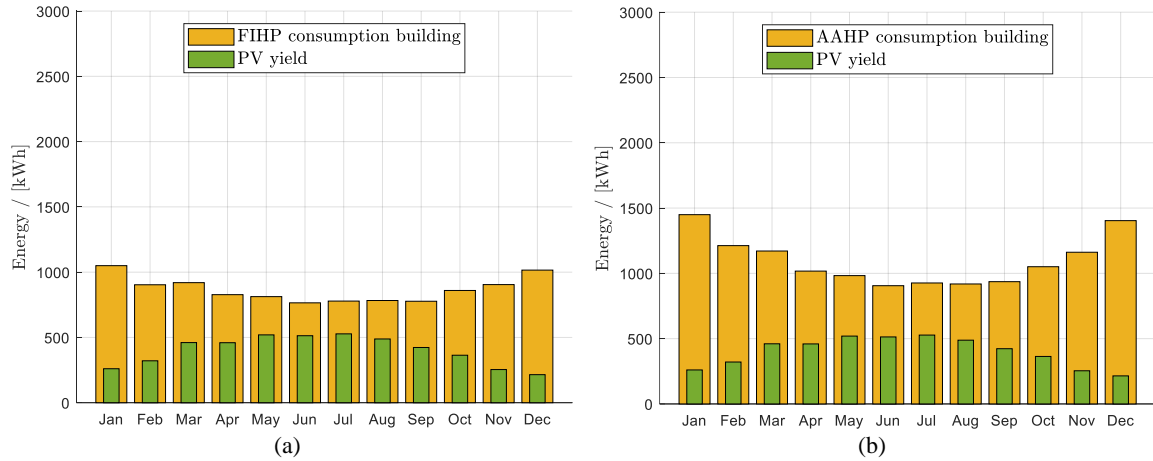


Figure 17: Simulated monthly electricity consumption for DHW preparation in the reference building and PV yield for (a) a mini-split façade-integrated HP and (b) a ducted air-source HP.

4. Conclusions

In this work, a comparative analysis of decentral systems for DHW preparation was performed. The results of the experiments indicated that common air-source boiler HPs available on the market have reduced heating capacities, which result in longer charging intervals and increased electricity consumption. Moreover, if such HPs are used as ambient air HPs, thermal losses further decrease the overall performance, with a COP_{DHW} of 1.28 at 10 °C ambient air temperature, 1.53 at 15 °C and 2.85 at 20 °C. An improvement can be reached with a return flow HP, which uses the return of the space heating as heat source. For this HP concept a COP_{DHW} ranging between 5.61 and 6.24 was measured for source temperatures of 25 and 35 °C respectively. However, this solution is highly dependent on the level of renovation of the heating system, which in turn has a huge impact on the invasiveness. A mini-split façade-integrated HP developed within the FFG-funded research projects *FitNeS* and *PhaseOut* can be a promising and efficient solution in renovated flats. For a source temperature of 10 °C a COP_{DHW} of 2.82 was measured, while at 15 °C and 20 °C COPs of 3.06 and 3.11 were reached, indicating a clear advantage compared to ambient air HPs. A simulation study was conducted to assess the yearly performance of the mini-split air-to-water HP compared to a ducted air-source boiler HP in a reference building with 10 renovated flats. A yearly PF of 2.50 was observed for the solution with the mini-split HP, while a PF of 1.99 was obtained for the solution with the ducted air-source HP. The gap in the performance is once again to be attributed to the lower heating capacity of the ducted air-source HP, which leads to longer charging intervals and larger electricity consumption. With a 5 kW peak PV system, a yearly coverage factor of about 50% could be reached for the system with the mini-split HP, while a coverage factor of only 37% was obtained for the ducted air-source HP with the same PV size. From these analyses, it can be concluded that the developed mini-split façade-integrated HP can be a viable and efficient solution in renovated multi-family buildings, where no disruptive construction works can be carried out and has a better performance than conventional air-source boiler HPs available on the market. In future work, the simulation study will be extended to the return-flow HP, for which the achieve building quality and the renovation degree of the SH system are crucial and for which different renovation scenarios will be evaluated. Furthermore, the optimal PV size to cover 50% and 60% of the electricity consumption for DHW will be investigated for all three presented HP concepts by means of parametric analyses.

5. Acknowledgments

This work has been part of the research projects “FitNeS” (FFG-Nr. 867327) and “PhaseOut” (FFG-Nr. 999895470) funded by the FFG (Austrian Research Promotion Agency) in the “Stadt der Zukunft” program. Our thanks go to the project partners Drexel und Weiss, Drexel Reduziert, Element Design, Winter, Rothbacher, Kulmer Holzbau and IIG.

6. References

- CEN/TC 113, 2017. EN 16147. Heat pumps with electrically driven compressors - Testing, performance rating and requirements for marking of domestic hot water units. <https://doi.org/https://dx.doi.org/10.31030/2513808>
- Cozza, S., Chambers, J., Bolliger, R., Tarantino, M., Patel, M.K., 2022. Decarbonizing residential buildings with heat pumps: Transferability of front-runner experiences from Swiss Cantons. *Energy Reports* 8, 14048–14060. <https://doi.org/10.1016/j.egy.2022.09.141>
- European Commission, 2021. Proposal for a Directive of the European Parliament and of the Council on the energy performance of buildings (recast). Official Journal of the European Union 0426.
- FFG (Austrian Research Promotion Agency), 2024. PhaseOut - Wärmepumpentechnologien in der Bestandssanierung [WWW Document]. URL <https://projekte.ffg.at/projekt/4499093> (accessed 7.17.24).
- FFG (Austrian Research Promotion Agency), 2023. FitNeS - Façade-integrated modular split heat pumps for new buildings and refurbishments [WWW Document]. URL <https://projekte.ffg.at/projekt/3037619> (accessed 8.8.24).
- Gustafsson, M., Dipasquale, C., Poppi, S., Bellini, A., Fedrizzi, R., Bales, C., Ochs, F., Sié, M., Holmberg, S., 2017. Economic and environmental analysis of energy renovation packages for European office buildings. *Energy Build* 148, 155–165. <https://doi.org/10.1016/j.enbuild.2017.04.079>
- IEA, 2022. The Future of Heat Pumps. The Future of Heat Pumps. <https://doi.org/10.1787/2bd71107-en>
- Mathworks, 2022. MATLAB [WWW Document]. URL <https://de.mathworks.com/products/matlab.html>
- Monteleone, W., Ochs, F., 2023. Simulation-assisted development of a mini-split air-to-water façade-integrated heat pump for minimal invasive renovations. 14th IEA Heat Pump Conference, Chicago.
- Monteleone, W., Ochs, F., Dermentzis, G., Breuss, S., 2024. Simulation-assisted design of a silent façade-integrated R290 mini-split heat pump. *Appl Therm Eng* 243, 122520. <https://doi.org/10.1016/j.applthermaleng.2024.122520>
- Ochs, F., Monteleone, W., Dermentzis, G., Siegele, D., Speer, C., 2022. Compact Decentral Façade-Integrated Air-to-Air Heat Pumps for Serial Renovation of Multi-Apartment Buildings. *Energies* (Basel) 15. <https://doi.org/10.3390/en15134679>
- Solar-Institut Juelich FH Aachen, 2018. CARNOT Toolbox.
- The European Parliament and the Council of the European Union, 2009. DIRECTIVE 2009/125/EC of the European Parliament and of the Council of 21 October 2009 establishing a framework for the setting of ecodesign requirements for energy-related products (recast) (OJ L 285 31.10.2009, p. 10). Official Journal of the European Union 1–40.